Proceedings of 2019 IEEE
International Conference on Mechatronics and Automation
August 4 - 7, Tianjin, China

2-DOF Haptic Device based on Closed-loop EBA Controller for Gastroscope Intervention

Zhaoyang Xue[1,3,4], Chongyang Wang[3,4,5], Xiao He[3,4,5]
Tao Yu[3,4,5], Xinyu Dong[2,3,4] and Hao liu[3,4,5*]

1. *Control engineering, Northeastern University, Shenyang, China*
2. *Shenyang Ligong University, Shenyang, China*
3. *State Key Laboratory of Robotics, Shenyang Institute of Automation, Chinese Academy of Sciences, Shenyang, China*
4. *Institutes for Robotics and Intelligent Manufacturing, Chinese Academy of Sciences, Shenyang, China*
5. *Key Laboratory of Minimally Invasive Surgical Robot, Liaoning Province, China*

xuezhaoyang@sia.cn
liuhao@sia.cn

***Abstract* - Force perception plays an indispensable role in the surgical process and will be of great value in the medical field. It has a significant impact on the quality, efficiency and safety of surgery. The main purpose of this research is to design, control and evaluate a haptic device. An improved method of the output force is proposed, which based on the structure of the 2-DOF joystick consisting of motors, drives and sensors. The improved Energy-bounding algorithm (EBAC) is designed to output stable torque while considering static compensation. In order to compare the performance of three methods of Torque-control algorithm (TCA), Energy-bounding algorithm (EBA) and the EBAC, a virtual wall test is conducted in CHAI3D. The test results show that the EBAC has good real-time performance and reliability. The calculating precision of device is 0.03 mm, the workspace is 200 mm and the output force is within 10.6 N (continuous force) and 42.4 N (peak force).**

Index Terms - haptic device. Energy-bounding algorithm. virtual wall test. CHAI3D.

I. INTRODUCTION

Gastro-intestinal (GI) disease is the most common type of disease in the clinic. The endoscope is a dependable diagnostic tool for the disease. Gastroscopic intervention is the use of a flexible endoscope through the esophagus into the stomach. The doctor judges whether there are ulcers or polyps at the esophagus, stomach and duodenum according to the images taken by camera at the end of the gastroscope. A robot-assisted master-slave system for gastroscope intervention had been developed to assist the operator [1]. It enables the intuitive projection of motion between gastroscope and joystick by remotely controlling the forward/backward, bending and rotating operation of the end of the gastroscope through the joystick, reducing the difficulty of operation. However, the doctor can only rely on the visual information provided by the camera for the operation without the haptic information. Therefore, the 2-DOF haptic device that could be equipped to the system needs to be developed, which not only provides a sense of force to the doctor but also guarantees that the gastroscope does not harm the tissue of a patient.

In the neuroscience and psychology prose, haptic is the study of human touch sensing. More precisely human touch can be classified as two kinds: (i) force and (ii) tactile information [2]. Force feedback means the direction force from different objects and boundaries, the weight of the grip or grip object, the mechanical compliance and inertia of the object; tactile information, which means skin sensation, allows the user to feel the temperature, compliance, structure, texture changes, pressure and vibration. Since the difficulty in identifying tactile information, currently, the developed system only considers force feedback and ignores tactile information.

Many scholars have studied in haptic devices for a long time. Berkelman and Hollis [3] have proposed an interesting design controlled by a magnetic field. But the device is not stable enough due to magnetic levitation control and has limited working space (the rotation is 14–20 degrees and the translation is 25 mm). The PHANTOM (Sensable Technologies) [4] has a 6-DOF wire-driven mechanism with a serial-parallel hybrid mechanism. However, high output forces are difficult to achieve using a tandem mechanism. Delta et al. [5] evaluate the 3-DOF Delta parallel robot. The Force Dimension Omega [6] is a kind of haptic device, which achieves output force, high stiffness, low inertia, and high back-drivability using the structure of DELTA parallel mechanisms. Yet, these mechanisms are complex in structure and large in size.

Considering the impedance control is the most widely used control design for the tactile interactions. The model is named “open-loop impedance control” [7] and it is used with PHANTOM. The open loop can maintain a certain precision but the accuracy is usually low and there is no automatic correcting ability. Furthermore, the position signal is not as sensitive as the current signal. Kim and Ryu [8] have proposed the EBA, which uses the damping element to consume the energy generated by the operator to ensure that the system is passive. The proposed algorithm guarantees robustly stable in haptic interactions.

2-DOF haptic devices with precise force and large working space have been developed to improve the current haptic feedback technology. The method is to add a force output based on the structure of the joystick, which not only maintains the flexible operation of the joystick but also has a real force output. The torque control system is designed to output stable torque while considering static compensation. Based on the approach of the EBA, the closed-loop controller is implemented using the position X acquired by the encoder and the force measured by the FT sensor as the feedback amount. Furthermore, the haptic device plays an important role in medical surgery and is urgently needed in the field of surgical operation. In various operations, surgeons perform

operations based on force feedback from patients. Telepresence is very helpful to doctors to avoid unnecessary injury, and improve the safety of operation.

The structure of this paper is as follows. The hardware, current calculation and software of the haptic device are described in Section II. Section III presents the torque control and the improved energy-bounding algorithm. Section IV presents experiments based on the different control methods and discussions, and conclusions and directions for future work are summarized in Section V.

II. HAPTIC DEVICE

A. Haptic Hardware

The torque used is provided by the motor. First, it is very important to ensure the safety of the equipment. The motor requires more power than most of the commercial devices. So, the maximum continuous current needs to be as large as possible. When the motor is overdriven in a short time, users will not worry about heating, combustion, etc. Second, in order to acquire the best quality of haptic fidelity, the coreless motors are chosen, so there is no cogging torque and the haptic device will be operated smoothly. By consulting motor manuals, the motor of RE30 meets our requirements. The stall current of the selected motor is 7.45 A, and the maximum continuous current is 1 A.

High tactile fidelity of the haptic devices needs to consider these non-ideal factors: the friction will weaken the haptic perception, the backlash causes the motors and the equipment to tremble, the structural compliance can lead to loss of ability to sense the stiff environments, and the equipment inertia [9]. The haptic device transmits torque through the wire to the handle and is not completed by the gear drive. The device is completed with two high-quality motors (Maxon RE30) with premounted encoders, and each motor drives the corresponding degree of freedom. CANopen is used as a communication interface. The 2-DOF device is configured for kinesthetic lively haptic feedback on the X and Y axis from measuring the real-time direction and position using an encoder. The haptic device is mainly made of aluminum. The device weighs approximately 1.7 kg, much smaller than a typical haptic equipment's weight requiring high power and large workspace. The haptic device is shown in Figure 1.

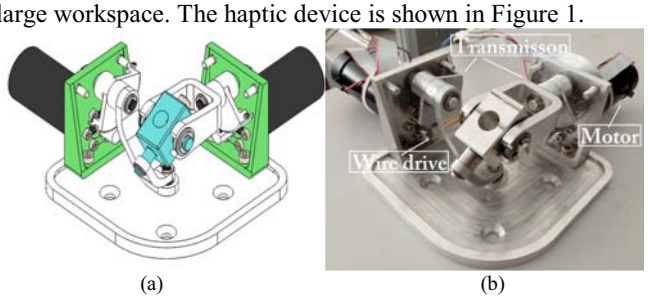

(a) (b)

Fig. 1 The model and object of the device.
(a) A solid design. (b) The actual metal assembly.

B. Current Calculation

The torque of the motor used is not related to the voltage supplied, but proportional to the current passing through it. However, Copley drives [10] can not measure the actual torque applied to the motor, so they cannot directly control the torque. Instead, the drives achieve motor control by adjusting the commanded current. To convert the torque command into a current command in Amps, the following calculation is made in Copely drives:

$$I = 0.001\,T\,T_C\,/\,T_S \tag{1}$$

Where I is the current output in Copley. T is the actual torque command. T_C is the continuous torque rating in units of 0.00001 Nm. T_S is the motor's torque constant in units of 0.00001 Nm/A.

The RE30 motor has a rated torque of 0.053 Nm and the torque constant of 0.0538 Nm/A. When the torque command is set to 500, the motor will output torque of the half of the motor's continuous torque. As a result, to specify a torque of 0.0265 Nm, the drive will output current of 0.4926 A. The amp will perform an operation to determine the current required.

C. Haptic Software

A virtual wall test system for a 2-DOF haptic device is given in Figure 2. In the first step, the position and speed of the manual operation are obtained in real time by the motor encoder. In the second step, the value of the encoder is read by the Copley driver and applied to the virtual object in CHAI3D [11] to define position and velocity. Then in the third step, if a collision occurs, the force information is updated by the controller, otherwise only the static compensation and the position data are converted.

The CHAI3D is an SDK based on C++, which can be used to develop a 3D virtual environment (VE) and define virtual interactions in the 3D VE. The haptic device is fed back to the operator. It allows you to quickly enter the virtual environment you want and provides a good experimental platform for different purposes of haptic testing. CHAI3D provides a new way of thinking for the development of force/tactile feedback control through the close integration of object haptic and visual perception and the abstraction of the complexity of personal haptic devices. The virtual wall test interface based on CHAI3D is developed.

The minimum necessary to use this device compulsory a PC with 2.5GHz i5-8300H CPU under windows 7 environment. Programming language required is visual C++. The compiler uses visual studio 2010. CHAI3D is used for graphics test and haptic rendering. And the data analysis requires Matlab R2014a.

III. THE INTERACTION FORCE CONTROL SCHEME

A. Torque Control Algorithm

The primary Torque control algorithm (TCA) achieved here has feedback control of a statically compensated torque scheme. According to (1), the algorithm is essentially the control of the current loop.

$$\tau_C = \tau_{static} + [F_D + K_p(F_D - F_M) + K_d(\dot{F}_D - \dot{F}_M)] \tag{2}$$

Where τ_C is the desired torque vector, which is converted to I by parameter K and sends to the motors, τ_{static} is the

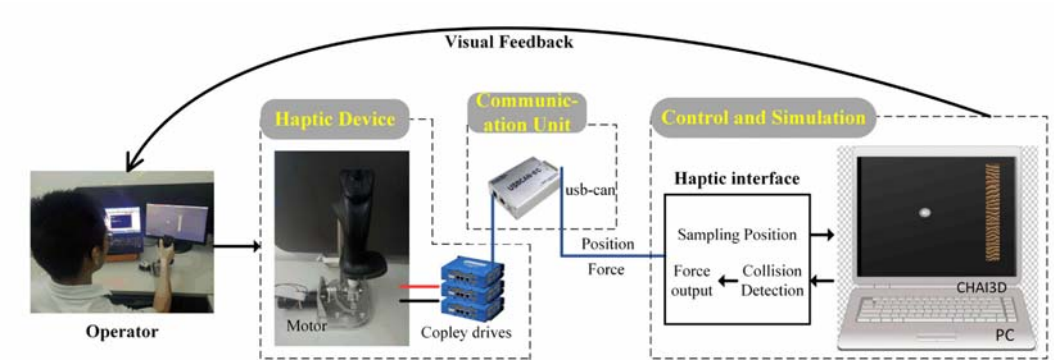

Fig. 2 The simulation system of haptic interaction.

inertia force, gravity and friction compensation vector, K_p and K_d are the matrices of PD coefficients, F_D is the desired torque vector at the end-effector, and, finally, F_M is torque vector measured by FT sensor. The controller design diagram is shown schematically in Figure 3.

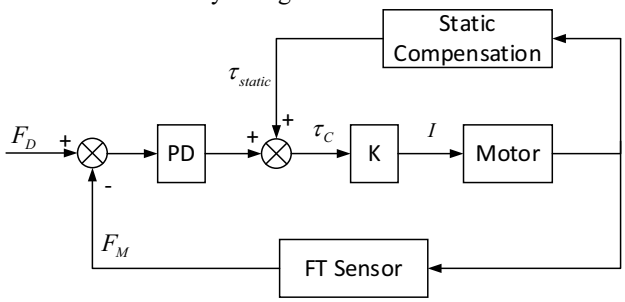

Fig. 3 Motor schematic control loop.

The haptic device should output high-quality haptic fidelity to user. The torque control scheme aims to offset the weight of the handle device by considering a static compensation, i.e. τ_{static}. This article [12] presents a practical and simple method for torque adjustment. This method gives a quasi-optimal coefficient set based on the system's step response.

B. Energy-bounding Algorithm

The Energy-bounding Algorithm (EBA), which ensures robustly stable haptic interactions, had been proposed and demonstrated by Kim and Ryu [8]. Based on their two-channel haptic control block diagram, we propose to implement closed-loop control by using the position acquired by the encoder and the force measured by the FT sensor. This will increase the stability of the system. The haptic interaction system consists of a human operator, haptic device, EBA controller and environment, the system is shown in Figure 4.

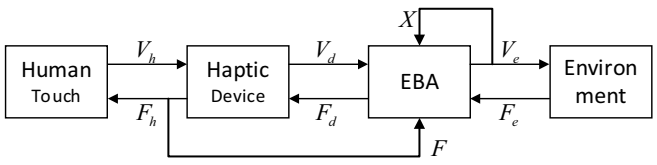

Fig. 4 The network representation of a haptic interaction system.

In Figure 4, V_h and F_h represent the velocity and force of the human touch, V_d and F_d represent velocity and command force of the haptic device, finally V_e and F_e represent velocity and expected rendering force of the virtual environment. If the entire haptic system is passive, the human operator and the remaining components must be passive at the frequency of interest, which meets the passive conditions as follows [13]:

$$\int_0^t F(\tau)^T V(\tau) d\tau + e(0) \geq 0 \quad t > 0 \text{, } all \text{ } function \text{ } F, V. \tag{3}$$

Where $e(0)$ is the initial energy stored by $t = 0$ in the system. When the human is not exposed to the virtual environment, consider model of human touch [14].

$$M_0 \dot{V}_h + B_0 V_h + K_0 (X_h - X_0) = F_h \tag{4}$$

$$V_h = \dot{X}_h \tag{5}$$

Where K_0, B_0 and M_0 are the effective stiffness, damper and mass of the combined human touch. The initial position X_h is 0 m and X_0 indicates the target location of the human operator's movement. Consider the force and velocity of the human touch from single-DOF device. From the network representation of a haptic system, the dynamics can be expressed as

$$F_h = M_h \dot{V}_h + B_h V_h + F_d \tag{6}$$

$$V_h = V_d \tag{7}$$

Where the effective mass and damper of the haptic device are M_h and B_h. When a human operator is exposed to the virtual environment, consider desired force that is computed from the virtual environment. For the model of tactile interaction, the energy bounding algorithm has following the control method [15]:

$$F_d(t) = F_d(t-1) + \beta(t) \mathrm{V}_d(t) \tag{8}$$

$$\beta(t) = (F_e(t) - F_d(t-1)) / V_d(t) \quad V_d(t) \neq 0 \tag{9}$$

Where $F_e(t)$ displayed to the operator is the desired force which is computed from the VE. The force difference $(F_d(t+1) - F_d(t))$ represents some energy dissipating elements, for example, damping components [12]. If the parameter $\beta(t)$ is within the bounds, then $F_d(t) = F_e(t)$ from

(8) and (9), entailing that the desired force $F_e(t)$ could be reflected to the human. But, they only analyse the boundary of $\beta(t)$, do not consider the effect on the continuity of $F_d(t)$, so we add this condition.

$$\begin{cases} \beta(t)=\beta_{\max} & \beta(t)>\beta_{\max} \\ \beta(t)=\beta_{\min} & \beta(t)<\beta_{\min} \\ \beta(t)=c_1\beta(t-1) & \beta(t)>c_1\beta(t-1), \beta_{\min} < \beta(t)<\beta_{\max} \\ \beta(t)=c_2\beta(t-1) & \beta(t)<c_2\beta(t-1), \beta_{\min} < \beta(t)<\beta_{\max} \end{cases} \tag{10}$$

And where c_1 and c_2 are positive constants satisfying $0.8 \le c_2 < 1 < c_1 \le 1.2$.

To show the availability of the EBAC, we numerically simulated the controller by using Matlab. Figure 5 demonstrates the stable interaction behavior of simulation experiments, and the desired position is set at 0.04 m. We choose a step size of 1 millisecond for the system. In particular, the plots in the first row show that the raised algorithm provided a stable and fast response. The plots in the second row are the actuator force $F_d(t)$. The plots in the third row give the change process $\beta(t)$ defined by (9).

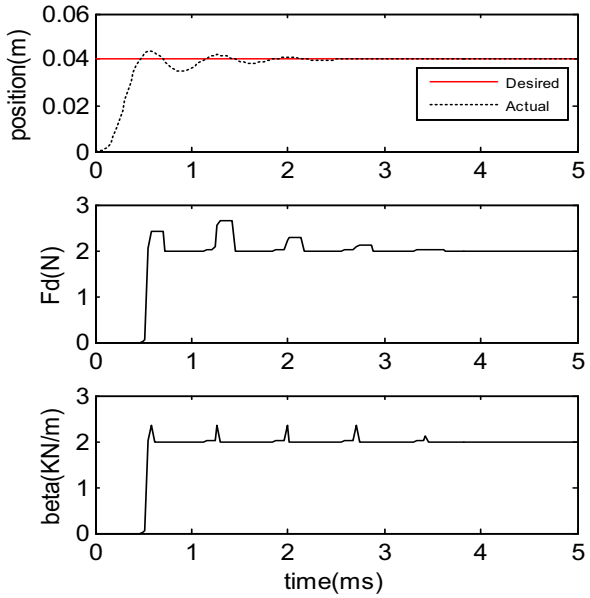

Fig. 5 Stable simulation results of the EBAC controller.

IV. Experiment and Discussion

A. Device Workspace

The working space of the operating device is the spherical surface with a radius (100 mm) of the joystick. Additionally, there is no singularity problem in the working space, and the mapping relationship is uniquely determined.

$$\begin{aligned} -30° < \theta_x < 30° \\ -30° < \theta_y < 30° \end{aligned} \tag{11}$$

Based on this workspace limitations, Figure 6 depicts the positional workspace for the 2-DOF customized haptic device as a 3D XYZ plot and then acquire the 2D XY plot, as shown in Figure 7. It has a large working space (200 mm in translation).

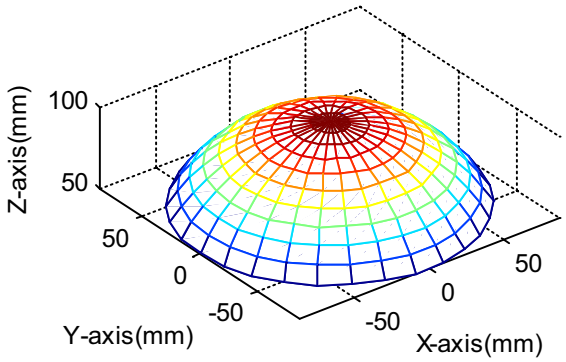

Fig. 6 2-DOF haptic device positional workspace 3D XYZ plot.

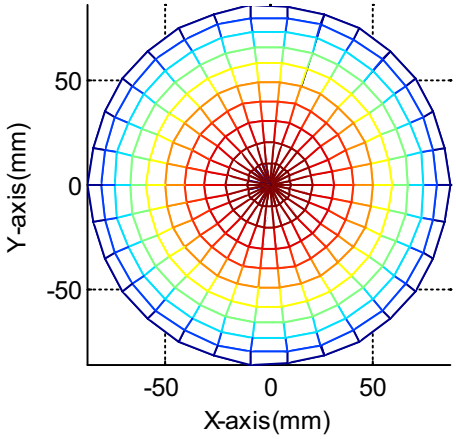

Fig. 7 2-DOF haptic device positional workspace 2D XY plot.

B. Device Evaluation

In order to assess the position sensitivity of the 2-DOF haptic device, pointing and tracking tasks are designed. The virtual ball in CHAI3D performs the corresponding motion according to the movement of the device in the control. The trajectories of the line and the circle are designed by us. In the first test, the operator moves the haptic device along a fixed ruler. Then, Figure 8 shows the result of experiment, red line in the figure represents the fitting result, while the black points indicate the real movement of the virtual ball. In the second test, the device makes a circular motion around a rope with a length of 80 mm and the result shows in Figure 9. Three sets of trajectory movement experiment have been completed, and some of the data are selected in each trajectory for the standard deviation (SD) calculation and the error of paths, respectively. Results are shown in Table I.

TABLE I

STANDARD DEVIATION AND ERROR VALUE OF THE TRAJECTORY

	Line			Circle		
SD(mm)	0.92	1.07	0.98	1.46	1.25	1.31
Error(mm)	0.78	0.89	0.86	0.93	0.91	0.97

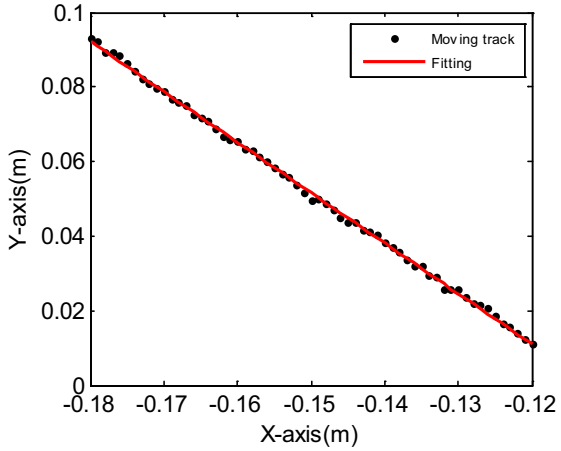

Fig. 8 Experimental results for the haptic device following a straight line.

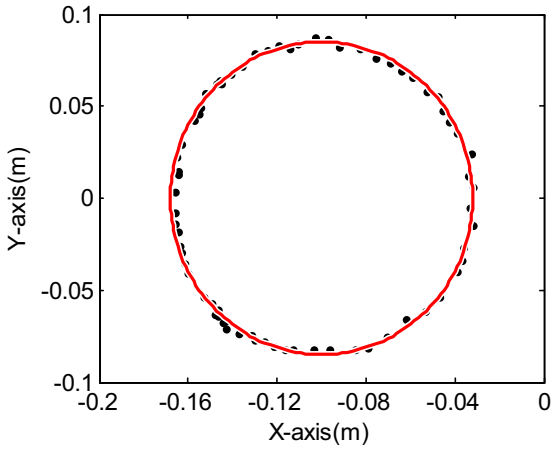

Fig. 9 Experimental results for the haptic device following a circle.

To the other properties, the device has a cable-driven capstan mechanism, whose maximum force output is 42.4 N, the continuous force output is 10.6 N, and the resolution of nominal position encoder is 0.03 mm as its basic specifications.

C. Virtual Wall Test

The so-called virtual wall is a combination of virtual reality technology and forces feedback technology to establish a virtual barrier for experimental devices. The experiment of the virtual wall is actually a one-dimensional force feedback experiment. The schematic diagram of the experiment is shown in Figure 10. Consider the mathematical model of a virtual wall.

$$\begin{cases} F = Kx + Bv & x \geq 0 \\ F = 0 & x < 0 \end{cases} \tag{12}$$

Where the K and B are the parameters of stiffness and damping representing the wall. The x is a shape variable. The v is a friction-related variable such as speed, positive pressure, and the like. And the position of the ball is mapped by the movement of the haptic device. The wall and ball present in the CHAI3D interface.

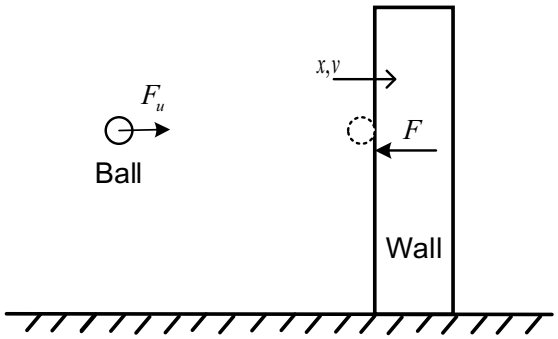

Fig. 10 Schematic diagram of the virtual wall.

To demonstrate the validity and stability of the improved Energy-bounding Algorithm, the virtual wall has been extensively tested. The simulation results with the same stiffness values (k=10kN m-1) using three different stability algorithms are shown in Figure 11. A basic algorithm (TCA) has huge oscillations. Although the approach can achieve force control through the PD controller, the feedback force fluctuates greatly. On the same stiffness wall experiment, the method of EBA proposed by Kim and Ryu leads to very poor performance. There is a stable deviation between the desired target position and the steady-state position. Compared with the controller of EBA, the EBAC can always get a stable response with higher display impedance. The position has no steady-state deviation, and the feedback force is realistic and stabilizes quickly.

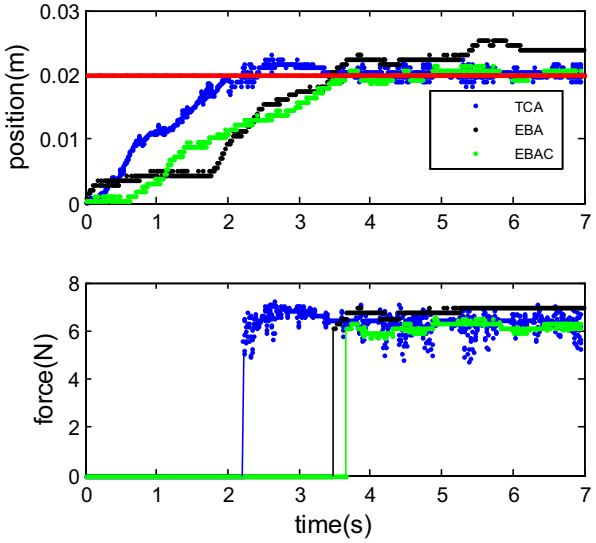

Fig. 11 Experimental results of different controller algorithms interacting with virtual walls.

The experiment of the virtual wall is one of the most basic experiments of 3D force feedback experiment [16], which shows the most basic elements and principles of force feedback. Extend the experiment to obtain a two-dimensional, three-dimensional or even multi-dimensional virtual force feedback scene.

D. Discussion

The error of the registration mainly comes from the following aspects. In the first place, there are deviations in the installation of the 2-DOF haptic device. Such as, inaccurate precision of the aluminum fittings and the difficulty in controlling the tightness of the wire rope. All of these will result in slight gaps in the handle and make the operation inaccurate. Secondly, the encoder is not accurate enough. The position encoder of the motor is 10 bits and the radius of the bearing is 5 mm, so the positional accuracy is calculated to be 0.03 mm. This can lead to insufficient positioning accuracy even affecting the controller deviation. Last but not least, the virtual wall simulated by the spring-mass model is not real enough, which is related to the values of stiffness, mass and damping.

V. Conclusion

In the context of gastroscope intervention robotics, it requires robots that could penetrate into the upper gastrointestinal. This ideal feature requires new technology to improve accuracy and safety interventions. Applying the improved method of EBAC to the 2-DOF haptic device can provide precise and stable interaction with the virtual environment. First, accuracy evaluations are conducted with actual tasks to validate the performance. The results show that the positional accuracy of the handle device can meet the surgical operation requirements. Further, experimental simulations are conducted with the virtual wall tests to compare the performance of three algorithms. According to the experimental data analysis, the improved control algorithm not only can enhance the position movement but also can output stable interaction force to ensure the quality of tactile mapping. However, the experiment is only conducted with virtual tasks in CHAI3D. The future research will attempt to study 3-DOF force feedback experiments, optimize its performance and combine with the robot system of gastroscope intervention.

Acknowledgment

This works is supported by the National key research and development plan (2018YFC0115101, China), NSFC (National Nature Science Foundation of China) programs (61873257) and the Self-planned Project from Institutes for Robotics and Intelligent Manufacturing (Y87B030101, China). The author thanks all members of the Intra-Lumenal Surgical Robotic Lab, especially Lei Cao and Jianhua Li, for their great help.

References

[1] Y. Li, H. Liu, S. Hao, et al, “Design and control of a novel gastroscope intervention mechanism with circumferentially pneumatic−driven clamping function,” *International Journal of Medical Robotics and Computer Assisted Surgery*, vol. 13, no. 1, pp. 7780-7783, March 2017.

[2] K. Salisbury, F. Conti, and F. Barbagli, “Haptic rendering: introductory concepts,” *IEEE computer graphics and applications*, vol. 24, no. 2, pp. 24-32, March 2004.

[3] P. J. Berkelman, R. L. Hollis, and S. E. Salcudean, “Interacting with virtual environments using a magnetic levitation haptic interface,” *IEEE/RSJ International Conference on Intelligent Robots and Systems. Human Robot Interaction and Cooperative Robots*. 2002, pp. 117-122.

[4] A. J. Silva, O. A. D. Ramirez, and V. P. Vega, “Phantom omni haptic device: Kinematic and manipulability,” *Electronics, Robotics and Automotive Mechanics Conference (CERMA)*, 2009, pp. 193-198.

[5] S. D. Stan, M. Manic, C. Szep, and R. Balan, “Performance analysis of 3 DOF Delta parallel robot,” *International Conference on Human System Interactions*, 2011, pp. 215-220.

[6] Z. Najdovski and S.Nahavandi, “Extending Haptic Device Capability for 3D Virtual Grasping,” *International Conference on Human Haptic Sensing and Touch Enabled Computer Applications. Springer, Berlin, Heidelberg*, 2008, pp. 494-503.

[7] C. R. Carignan and K. R. Cleary, “Closed-Loop Force Control for Haptic Simulation of Virtual Environments,” *Haptics-e, The Electronic Journal of Haptics Research*, vol. 1, no. 2, February 2000.

[8] J. P. Kim, J. Ryu, “Robustly Stable Haptic Interaction Control using an Energy-bounding Algorithm,” *The International Journal of Robotics Research*, vol. 29, no. 6, pp. 666-679, May 2010.

[9] M. Yip, J. Forsslund, “Spurring Innovation in Spatial Haptics: How Open-Source Hardware Can Turn Creativity Loose,” *IEEE Robotics & Automation Magazine*, vol. 24, no. 1, pp. 65-76, March 2017.

[10] Maxon.[Online].Available:https://www.copleycontrols.com/support

[11] CHAI3D. (2014). [Online]. Available: http://www.chai3d.org

[12] L. Birglen, C. Gosselin, et al. “SHaDe, A New 3-DOF Haptic Device,” *IEEE Trans on Robotics & Automation*, vol. 18, no. 2, pp. 166-175, August 2002.

[13] J. E. Colgate, and G. G. Schenkel, “Passivity of a class of sampled-data systems: Application to haptic interfaces,” *Journal of robotic systems*, vol. 14, no. 1, pp. 37-47, January 1997.

[14] N. Hogan, “Controlling impedance at the man/machine interface,” *IEEE International Conference on Robotics and Automation*, 1989, pp. 1626-1631.

[15] J. P. Kim, C. Seo, J. Ryu, “A Multirate Energy Bounding Algorithm for High Fidelity Stable Haptic Interaction Control,” *International Joint International on Sice-icase*, 2006, pp. 215-220.

[16] K. Kiguchi, T. Hora, “A Virtual Wall for Perception-Assist with a Lower-Limb Power-Assist Robot,” *Third International Conference on Computing Measurement Control and Sensor Network*, 2016, pp. 104-109.